METALLURGICAL TECHNOLOGIES / **МЕТАЛЛУРГИЧЕСКИЕ ТЕХНОЛОГИИ**

A STUDY ON PROCESSING OF BLAST FURNACE DUST AND SLUDGE USING REDUCTION ROASTING AND MAGNETIC SEPARATION

P. I. Grudinsky[1] ✉, A. A. Yurtaeva[1], A. I. Volkov[2], V. G. Dyubanov[1]

[1] **Baikov Institute of Metallurgy and Materials Science, Russian Academy of Sciences** (49 Leninskii Ave., Moscow 119334, Russian Federation)
[2] **I.P. Bardin Central Research Institute of Ferrous Metallurgy** (23/9 Radio Str., Moscow 105005, Russian Federation)

✉ pgrudinskiy@imet.ac.ru

Abstract. Blast furnace dust and sludge are by-products of ironmaking that contain high levels of iron and carbon, along with zinc. The increased zinc content complicates their recycling in the sintering and blast furnace processes, leading to their accumulation in waste dumps. This study investigates different treatment methods for recovering valuable elements from blast furnace dust (BFD) and blast furnace sludge (BFS) through reduction roasting and magnetic separation. Thermodynamic calculations and laboratory experiments were conducted to evaluate three approaches: magnetic separation without the roasting, as well as roasting stages to reduce iron to magnetite at 800 °C or metallic iron at 1200 °C, respectively. Direct magnetic separation without roasting and with the preliminary roasting at 800 °C resulted in magnetic concentrates of 49 – 63 % Fe from the BFD and BFS samples, but with elevated zinc content. The best results were achieved using reduction roasting at 1200 °C for 120 min, followed by grinding the samples to –0.054 mm and magnetic separation with a magnetic field of 0.1 T. As a result, the metallized magnetic concentrate containing 73.8 % Fe and 0.048 % Zn was obtained from the BFS sample (initially containing 39.5 % Fe and 0.31 % Zn), while a concentrate containing 80 % Fe and 0.019 % Zn was produced from the BFD sample (initially containing 44.6 % Fe and 0.31 % Zn). The iron recovery into the concentrates for the BFS and BFD samples was 92.8 and 89.7 %, respectively. The proposed approach can produce valuable materials for ferrous and non-ferrous metallurgy from these by-products, increase the efficiency of sintering and blast furnace processes, and reduce waste accumulation.

Keywords: blast furnace dust, blast furnace sludge, processing, reduction roasting, magnetic separation, carbothermic reduction, iron, zinc

ИССЛЕДОВАНИЕ ПРОЦЕССОВ ПЕРЕРАБОТКИ ДОМЕННЫХ ПЫЛИ И ШЛАМА С ИСПОЛЬЗОВАНИЕМ ВОССТАНОВИТЕЛЬНОГО ОБЖИГА И МАГНИТНОЙ СЕПАРАЦИИ

П. И. Грудинский[1] ✉, А. А. Юртаева[1], А. И. Волков[2], В. Г. Дюбанов[1]

[1] **Институт металлургии и материаловедения им. А.А. Байкова РАН** (Россия, 119334, Москва, Ленинский пр. 49)
[2] **Центральный научно-исследовательский институт черной металлургии им. И.П. Бардина** (Россия, 105005, Москва, ул. Радио, 23/9)

✉ pgrudinskiy@imet.ac.ru

Аннотация. Пыли и шламы доменного производства – техногенные материалы с высоким содержанием железа и углерода, в которых присутствует также цинк. Повышенное содержание цинка препятствует их рециклингу в агломдоменном переделе и приводит к накоплению этих материалов в отвалах. В настоящей работе исследованы различные варианты переработки образцов доменной пыли (ДП) и доменного шлама (ДШ) с извлечением ценных элементов на основе восстановительного обжига и магнитной сепарации. С помощью термодинамических расчетов и лабораторных экспериментов изучены три варианта реализации этого способа: магнитная сепарация без предварительного обжига, а также со стадиями обжига с восстановлением железа до магнетита при 800 °С и металлического железа при 1200 °С соответственно. Способы прямой магнитной сепарации без обжига и с предварительным обжигом при 800 °С позволяют получить из образцов ДП и ДШ магнитные концентраты с 49 – 63 % Fe, но содержание цинка в них остается повышенным. Лучшие результаты были получены с использованием восстановительного обжига при 1200 °С продолжительностью 120 мин, последующего размола образцов до –0,054 мм и магнитной сепарации при индукции магнитного поля 0,1 Тл. В результате из ДШ, содержащего 39,5 % Fe и 0,31 % Zn,

получен металлизованный магнитный концентрат с содержанием 73,8 % Fe и 0,048 % Zn, а из ДП, содержащей 44,6 % Fe и 0,31 % Zn – металлизованный магнитный концентрат с содержанием 80 % Fe и 0,019 % Zn. Степень извлечения железа в концентрат для ДШ и ДП составила 92,8 и 89,7 % соответственно. Предложенный подход позволяет получать ценные материалы для черной и цветной металлургии из техногенного сырья, увеличить эффективность агодоменного передела и избежать накопления отходов.

Ключевые слова: доменная пыль, доменный шлам, переработка, восстановительный обжиг, магнитная сепарация, карботермическое восстановление, железо, цинк

INTRODUCTION

Dust and sludge generated in blast furnace ironmaking are by-products with high iron content collected in dry and wet gas cleaning systems, respectively. The production of such dust and sludge ranges from 5.5 to 40 kg/t of hot pig iron [1]. The conventional method for their recycling is sintering followed by blast furnace processing. However, the recycling through the sintering and blast furnace route becomes complicated when zinc content in these materials increases causing technological difficulties in the blast furnace smelting process [2]. When the dust or sludge contains >0.05 % Zn, the recycling in the sintering process becomes complicated; if the zinc content exceeds 0.3 – 0.5 % Zn, the recycling is nearly impossible [3]. In such cases, dust and sludge are dumped in landfills and classified as IV class hazardous waste leading to adverse environmental impacts near disposal sites.

Several studies have suggested that blast furnace dust and sludge can be recycled in the production of cement [4], ceramics [5], and road construction [6; 7]; however, these studies do not address the recycling of dust and sludge with high zinc content. Additionally, it is possible to use such dust and sludge as adsorbents [8; 9], catalysts [10; 11], and for coagulant production [12], but these applications can only utilize a small portion of the accumulated and generated waste. Various approaches have been explored for processing blast furnace dust and sludge [13] including the recovery of iron, carbon, zinc, and other valuable elements by hydrometallurgical, pyrometallurgical, and beneficiating methods. Hydrometallurgical processes using various solvents are often multistage [14], have low selectivity for separating zinc and iron [15], and make it impossible to recycle iron-containing residues rendering them inefficient for zinc contents <10 % [13]. Beneficiating methods for processing blast furnace dust and sludge include gravity concentration [16], air classification [17], flotation [18], magnetic separation [19], and their various combinations [20; 21]. These methods allow for selective separation of carbon and iron but struggle to segregate zinc into a separate product. In contrast, pyrometallurgical methods based on zinc reduction and evaporation enable selective separation of zinc from iron, with the carbon content in the dust and sludge serving as a reducing agent [22]. Therefore, combining pyrometallurgical and beneficiating methods is a promising approach for the comprehensive recovery of valuable elements from blast furnace dust and sludge.

In this study, we explore a method for processing blast furnace dust and sludge based on carbothermic reduction roasting and magnetic separation, which has shown high efficiency for other materials containing zinc and iron [23; 24]. Based on thermodynamic calculations and laboratory experiments, we identified the characteristics of three variations of this method: without roasting, with roasting to reduce iron to magnetite, and with roasting to reduce iron to its metallic form. Based on the research results, the prospects and directions for recycling of magnetic separation products were assessed.

MATERIALS AND METHODS

Samples of blast furnace sludge (BFS) and blast furnace dust (BFD) were obtained from PJSC NLMK (Lipetsk, Russia). Chemical analysis of the samples was carried out using a PANalytical AXIOS^{mAX} Advanced *X*-ray fluorescence spectrometer (Netherlands). The iron content in the samples was determined by redox titration according to GOST 32517-1-2013. Carbon and sulfur contents were measured using a LECO CS–400 analyzer (USA).

Mineralogical analysis of the initial samples was carried out with a DRON-3 diffractometer (Russia) using CuK_α radiation, while the magnetic separation products were analyzed with a Difrey diffractometer (Russia) using CrK_α radiation. *X*-ray diffraction (XRD) patterns were interpreted using the Match 3.15 software (Germany) [25].

Quantitative determination of divalent and metallic iron in the samples was conducted via redox titration, following the methods outlined in GOST 23581.3–79 and 26482–90, respectively. The proportion of ferric iron was calculated as the difference between Fe_{tot} and the sum of Fe_{met} and Fe^{2+}.

Thermodynamic calculations of the equilibrium states of iron and zinc compounds at the temperatures of the reduction roasting were performed using the Equilibrium composition module of the HSC Chemistry 9.9 software (Finland) [26]. The calculations were conducted in the temperature range of 300 – 1400 °C, under atmospheric pressure, with an inert atmosphere for 100 kg of blast furnace sludge (BFS) or blast furnace dust (BFD).

Laboratory experiments with BFS and BFD were carried out using three approaches: magnetic separation of the samples without the preliminary roasting, magnetizing roasting at 800 °C followed by magnetic separation, and metallizing roasting at 1200 °C followed by magnetic separation.

Magnetic separation of the samples ground to the required particle size was performed using an XCGS-50 wet tubular magnetic separator (China) with a magnetic field of 0.1 T. The separation process was conducted for the samples with coarse (–1 mm) and fine (–0.054 mm) grinding. A 10 g sample was placed in the separator, processed in tap water, and the resulting slurry was filtered using vacuum filtration with a suction flask and funnel. The separation products were then dried at 100 °C for 120 min. If needed, the products were further ground for additional analyses.

The magnetizing roasting of 50 g samples of BFS and BFD at 800 °C was carried out in a muffle furnace for 30 min. The samples were placed in corundum crucibles, inverted, and then positioned inside a larger corundum crucible. The roasting duration was selected based on literature data [27 – 29] indicating that full reduction of iron to magnetite in similar materials occurs within 30 min. After the roasting, the samples were removed from the furnace, quenched in water to prevent secondary oxidation of magnetite, filtered using a vacuum pump and suction flask, and dried at 100 °C for 120 min. The samples were subsequently ground and sieved to the required particle size.

The magnetizing metallizing roasting was conducted in a muffle furnace at 1200 °C for 120 min in a nitrogen atmosphere. Samples weighting 50 g were placed into corundum crucibles on a graphite layer with the +2.5 mm fraction, followed by another graphite layer on top. The temperature and roasting duration were selected with an excess margin to ensure complete iron metallization and zinc removal, based on literature data [30], where iron reduction and only trace zinc content from a similar blast furnace dust sample were achieved at 1200 °C for 100 min. The samples were heated to 1200 °C at a rate of 5 °C/min, held at this temperature for 120 min, and then cooled down to 200 °C over 900 min along with the furnace. The entire heating, holding, and cooling process was carried out in a nitrogen atmosphere (≥99.6 % N_2 and ≤0.4 % O_2) to prevent secondary oxidation of iron. Two experiments were conducted with the BFS and BFD

samples: one without any additives and the other with a 15 % excess of carbon. High-purity graphite was used as a carbon-containing reducing agent. After roasting, the samples were ground and sieve to the required size for subsequent magnetic separation.

The efficiency of roasting and magnetic separation processes was calculated using the following formulas:

$$\gamma_c = \frac{m_c}{m_0} 100 \ \%; \qquad (1)$$

$$\gamma_t = \frac{m_t}{m_0} 100 \ \%; \qquad (2)$$

$$\varepsilon_c = \frac{m_c \, \% \, \mathrm{Fe}_c}{m_0 \, \% \, \mathrm{Fe}_0} 100 \ \%; \qquad (3)$$

$$\varepsilon_t = \frac{m_t \, \% \, \mathrm{Fe}_t}{m_0 \, \% \, \mathrm{Fe}_0} 100 \ \%; \qquad (4)$$

$$\mu_0 = \frac{\% \, \mathrm{Fe}_{0(\mathrm{met})}}{\% \, \mathrm{Fe}_0} 100 \ \%; \qquad (5)$$

$$\mu_c = \frac{\% \, \mathrm{Fe}_{c(\mathrm{met})}}{\% \, \mathrm{Fe}_c} 100 \ \%; \qquad (6)$$

$$\xi_{\mathrm{Zn}} = \left(1 - \frac{m_r \, \% \, \mathrm{Zn}_r}{m_w \, \% \, \mathrm{Zn}_w}\right) 100 \ \%, \qquad (7)$$

where γ_c and γ_t is yield of magnetic and non-magnetic fractions, respectively, %; m_0 is initial mass of the samples for magnetic separation, g; m_c and m_t mass of magnetic and non-magnetic fractions obtained after magnetic separation, g; ε_c and ε_t is iron recovery in the magnetic and non-magnetic fractions, respectively, %; % Fe_0 is total iron content in the initial samples for magnetic separation, wt. %; % Fe_c and % Fe_t is total iron content in the magnetic and non-magnetic fractions, respectively, wt. %; μ_0 and μ_c is iron metallization degree in the initial samples for magnetic separation and magnetic fraction, respectively, %; % $\mathrm{Fe}_{0(\mathrm{met})}$ and % $\mathrm{Fe}_{c(\mathrm{met})}$ is metallic iron content in the initial samples for magnetic separation and magnetic fraction, respectively, %; ξ_{Zn} is zinc removal degree during roasting, %; % Zn_r and % Zn_w is zinc content in the roasted and initial samples, respectively, wt. %; m_r and m_w is mass the roasted and initial samples, respectively, g.

Zinc content in the samples was analyzed using an inductively coupled plasma atomic emission spectrometer (ICP-AES) Vista Pro (Australia). The zinc content in the form of ZnO was determined according to the procedure outlined in [31], which involved sample leaching in an aqueous solution of $NH_4Cl + NH_4OH$. A 0.5 g sample was placed in a conical flask containing 50 ml of the solution prepared by dissolving 22 g of NH_4Cl in a mixture of 80 ml of NH_4OH (density 0.9 g/cm³) and 120 ml of water. The solution and sample were stirred on a magnetic agita-

tor at 50 – 60 °C for 120 min, then filtered. The zinc content in the filtrates was then analyzed using the ICP-AES device.

RESULTS AND DISCUSSION

Table 1 presents the elemental composition of the BFS and BFD samples, while Fig. 1 shows the XRD patterns of the samples with the identified phases marked.

The main components of the BFS and BFD samples are iron and carbon. The iron content in BFD is higher than in BFS, whereas the carbon content is lower. The level of phosphorus and sulfur, which are the main harmful impurities in iron and steel metallurgy, along with other undesirable impurities such as arsenic and copper, are within acceptable limits for the recycling in sintering and blast furnace processes. However, the elevated zinc content, as shown in the data, poses a significant challenge for the recycling these wastes in iron and steel metallurgy.

As indicated by the XRD patterns, the primary minerals of both samples are hematite and magnetite, which are the main components of iron ore raw materials used in blast furnace operations. Metallic iron and wustite are present in significantly smaller quantities. Carbon in the samples is predominantly in the form of graphite, which originates from coke and enters the gas cleaning waste, along with a small amount of calcite. The high graphite content in the samples is advantageous for the reduction roasting process. It should be noted that an amorphous ring is present in both XRD patterns, likely due to the presence of blast furnace slag particles in the wastes. The BFS sample contains small amounts of hydrate minerals, such as ettringite and gypsum, which were likely formed during the wet gas cleaning process.

The analysis of iron form distribution in BFS and BFD revealed that the majority of iron in both the samples is in the trivalent form (Fe^{3+}), accounting for 90.9 % in BFS and 89.1 % BFD. Divalent iron (Fe^{2+}) constitutes 6.1 and 7.7 % of the iron in BFS and BFD, respectively, while metallic iron (Fe_{met}) accounts for 3.0 and 3.2 %, respectively. Therefore, the distribution of iron forms in BFS and BFD is quantitatively similar.

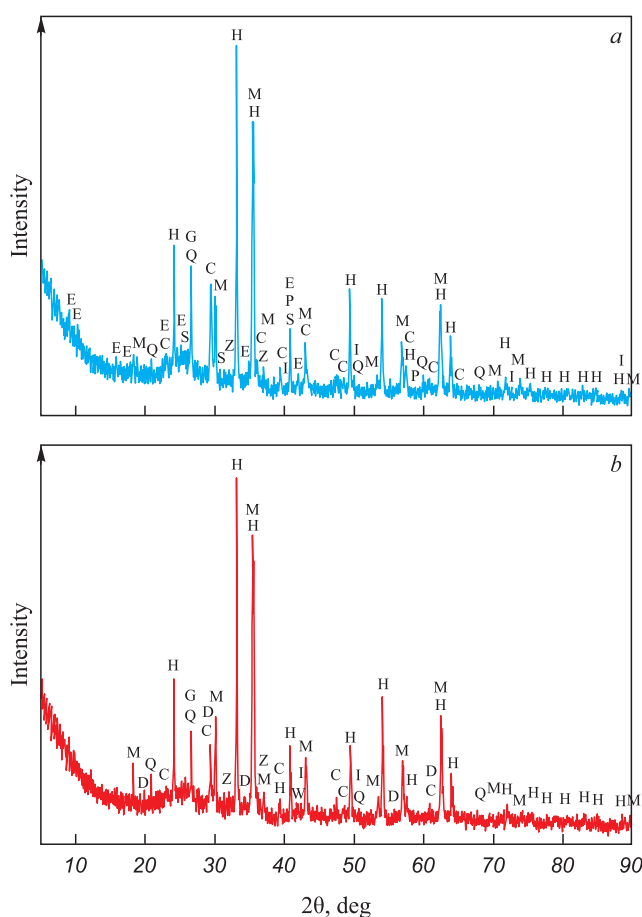The composition of the BFS and BFD used for thermodynamic calculation based on the results of chemical and mineralogical analyses and was adopted as follows, wt. %:

– BFS: 44.27 Fe_2O_3; 9.94 Fe_3O_4; 1.20 Fe; 21.43 C; 0.29 ZnO; 1.15 MgO; 6.11 SiO_2; 0.93 $CaSO_4$; 13.12 $CaCO_3$; 0.60 Al_2O_3; 0.26 $ZnFe_2O_4$; 0.21 $Ca(OH)_2$; 0.16 $Al_2(SO_4)_3$;

– BFD: 46.86 Fe_2O_3; 14.32 Fe_3O_4; 1.42 Fe; 14.97 C; 0.07 ZnO; 1.01 MgO; 5.75 SiO_2; 1.67 $CaMgSi_2O_6$; 11.91 $CaCO_3$; 0.81 $CaSO_4$; 1.11 Al_2O_3.

Fig 1. XRD patterns of BFS (*a*) and BFD (*b*):
H – hematite (α-Fe_2O_3); M – magnetite (Fe_3O_4); C – calcite ($CaCO_3$); G – graphite (C); Q – quartz (SiO_2); I – iron (α-Fe); W – wustite (FeO); E – ettringite ($Ca_6Al_2(SO_4)_3(OH)_{12}\cdot26H_2O$); D – diopside ($CaMgSi_2O_6$); P – periclase (MgO); Z – zincite (ZnO); S – gypsum ($CaSO_4\cdot2H_2O$)

Рис. 1. Дифрактограммы ДШ (*a*) и ДП (*b*):
H – гематит (α-Fe_2O_3); M – магнетит (Fe_3O_4); C – кальцит ($CaCO_3$); G – графит (C); Q – кварц (SiO_2); I – железо (α-Fe); W – вюстит (FeO); E – эттрингит ($Ca_6Al_2(SO_4)_3(OH)_{12}\cdot26H_2O$); D – диопсид ($CaMgSi_2O_6$); P – периклаз (MgO); Z – цинкит (ZnO); S – гипс ($CaSO_4\cdot2H_2O$)

Table 1. **Chemical composition of the BFS and BFD samples, wt. %**

Таблица 1. **Химический состав образцов ДШ и ДП, мас. %**

Waste	Fe	Zn	Al	Ca	Si	Mg	K	Mn	Cr	Cu	Ti	P	Pb	As	S	C
BFS	39.5	0.31	0.75	5.61	2.86	0.69	0.01	0.19	0.02	0.011	0.066	0.049	0.198	0.02	0.24	23.0
BFD	44.6	0.06	0.59	5.29	3.12	0.80	0.05	0.21	0.02	–	0.048	0.048	–	0.01	0.17	16.4

Fig. 2 illustrates the equilibrium amounts of iron and zinc compounds, as well as graphite in the system based on BFS and BFD at temperatures ranging from 300 to 1400 °C.

According to the data obtained, the reduction of iron to metal and the evaporation of metallic zinc are thermodynamically probable at temperatures above 700 °C. It should be noted that the amount of carbon in both samples is sufficient for the reduction of iron and zinc, although the BFD system contains a small amount of iron sulfide (Fig. 2, *c*). In the BFS system, the carbon content is more than sufficient, as evidenced by the presence of 7 – 10 kg of excess graphite at temperatures above 700 °C.

Literature data suggest that, contrary to thermodynamic calculations, favorable kinetic conditions for the carbothermic reduction of iron to metal only occur at temperatures above 1000 °C [32]. At temperatures of 700 – 900 °C, the magnetizing roasting with the carbothermic reduction of iron to Fe_3O_4 is possible [29]. These findings were taken into account in the experiments.

Table 2 lists the results of the analysis of the roasted samples obtained from BFS and BFD.

As shown in Table 2, the iron content in the samples after the roasting at 800 °C increases slightly. The content of metallic iron decreases due to its oxidation during the roasting. The degree of zinc removal in these samples is negligible, with only a slight change in the ZnO content.

After the roasting at 1200 °C, the iron content increases further, with most of the iron transforming into a metallic form. The iron content in the samples with an excess of carbon is lower than in the samples without the carbon addition, due to the presence of residual unreacted graphite. The degree of iron metallization in the samples ranges from 84 to 96 %. It is worth noting that the addition of carbon decreases the degree of iron metallization in the BFS sample, while it increases it in the BFD sample. The degree of zinc removal during the roasting is approximately 93 % for the BFS sample and 54 – 68 % for the BFD sample. The residual zinc content in the roasted samples is in the range of 0.02 – 0.04 % indicating that these roasted samples could potentially be used as part of the sinter burden without subsequent magnetic separation. Furthermore, the reduction roasting process can yield an additional valuable by-product: a sublimate with a high zinc content.

Table 3 shows the characteristics of the magnetic separation process for BFS and BFD samples, along the analysis results of the products.
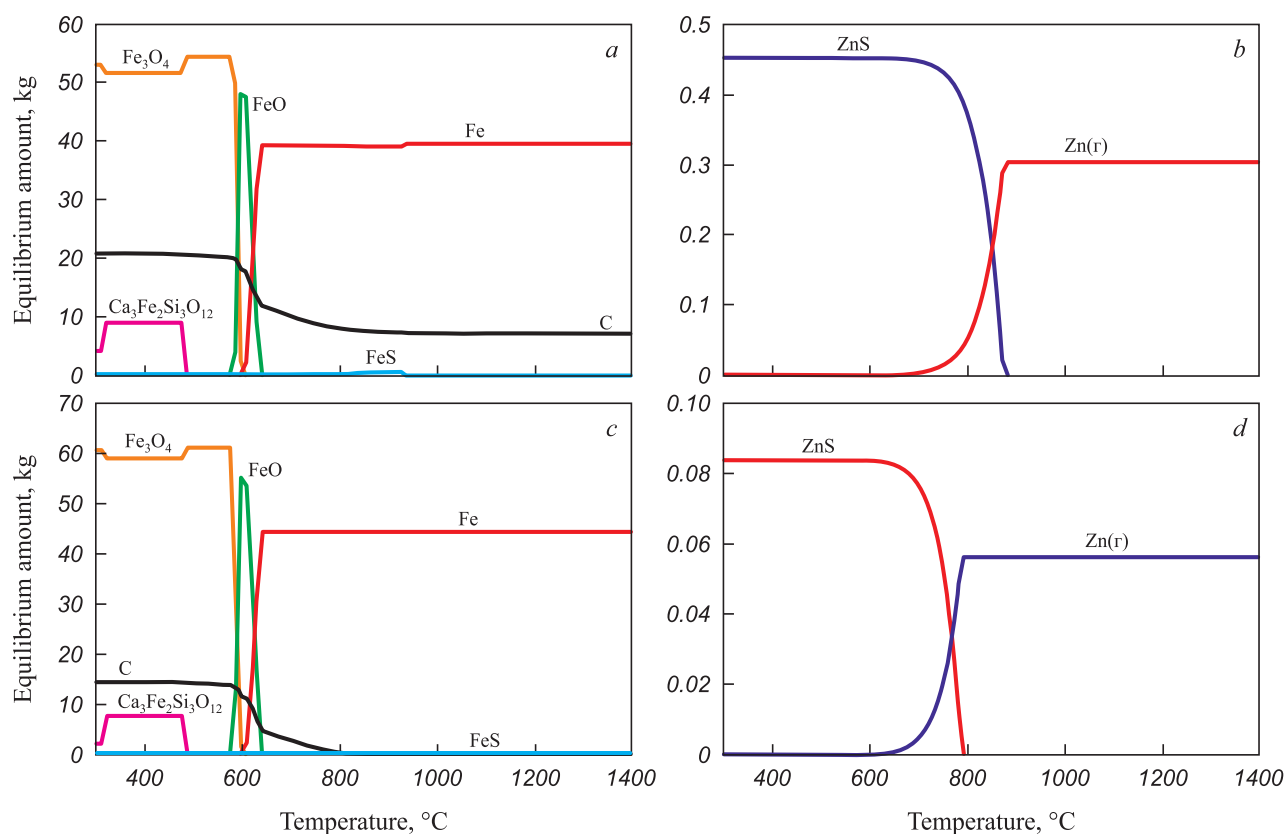

Fig. 2. Equilibrium amounts of graphite and iron compounds (*a*, *c*), as well as zinc compounds (*b*, *d*) in the BFS (*a*, *b*) and BFD (*c*, *d*) at 300 – 1400 °C

Рис. 2. Равновесные количества графита и соединений железа (*a*, *c*), а также соединений цинка (*b*, *d*) в ДШ (*a*, *b*) и ДП (*c*, *d*) при 300 – 1400 °C

Table 2. Chemical composition of the BFS and BFD samples and the products of their roasting at 800 and 1200 °C,
along with the zinc removal degree

Таблица 2. Химический состав ДШ и ДП и продуктов их обжига при 800 и 1200 °C,
а также степень удаления из них цинка

Initial sample	Roasting conditions	Content, wt. %			Zn removal degree (ξ_{Zn}), %	Fe metallization degree (μ_0), %
		Fe_{tot}	Zn_{tot}	Zn_{ZnO}		
BFS	No roasting	39.48	0.310	0.230	–	3.03
	800 °C, 30 min	41.16	0.320	0.210	1.0	2.03
	1200 °C, 120 min	59.18	0.030	n/d	93.2	90.4
	1200 °C, 120 min, + 15 % C	49.26	0.023	n/d	93.5	88.4
BFD	No roasting	44.56	0.060	0.055	–	3.19
	800 °C, 30 min	45.97	0.062	0.060	0.5	1.21
	1200 °C, 120 min	63.92	0.039	n/d	54.3	84.5
	1200 °C, 120 min, + 15 % C	58.02	0.023	n/d	68.2	96.2
N o t e: n/d – no data.						

Table 3. Yield, recovery degree and content of Fe and Zn in magnetic and non-magnetic fractions obtained
from BFS and BFD using magnetic separation, as well as roasting at 800 and 1200 °C followed by magnetic separation

Таблица 3. Выход, степень извлечения и содержание Fe и Zn в магнитной и немагнитных фракциях,
полученных из ДШ и ДП магнитным, а также обжиг-магнитным методами с обжигом при 800 и 1200 °C

Waste	Roasting conditions	Magnetic separation conditions	Fraction yield (γ), %		Fe recovery degree in the fraction (ε), %		Content in the fraction, wt. %			Fe metallization degree in magnetic fraction (μ_c), %
			magn.	non-magn.	magn.	non-magn.	magn.		non-magn.	
							Fe_{tot}	Zn	Fe_{tot}	
BFS	No roasting	0.1 T, –1 mm	35.30	58.90	45.7	50.30	51.1	0.260	33.70	9.34
		0.1 T, –0.054 mm	33.40	62.80	52.7	45.50	62.3	0.210	28.60	8.42
	800 °C, 30 min	0.1 T, –1 mm	79.50	17.90	97.3	2.05	51.4	0.390	4.73	9.62
		0.1 T, –0.054 mm	63.80	32.30	94.6	3.45	61.0	0.430	4.40	8.25
	1200 °C, 120 min	0.1 T, –1 mm	84.20	14.00	90.8	1.91	63.8	n/d	8.04	94.60
		0.1 T, –0.054 mm	74.40	22.50	92.8	4.00	73.8	0.048	10.50	88.90
	1200 °C, 120 min, + 15 % C	0.1 T, –1 mm	85.20	13.60	90.0	3.68	52.0	n/d	13.30	89.50
		0.1 T, –0.054 mm	63.30	36.20	84.2	8.69	65.6	0.048	11.80	88.70
BFD	No roasting	0.1 T, –1 mm	62.00	38.70	68.3	26.20	49.1	0.120	30.20	9.80
		0.1 T, –0.054 mm	45.60	50.80	63.4	35.00	63.0	0.070	28.60	8.08
	800 °C, 30 min	0.1 T, –1 mm	80.00	21.50	92.1	1.73	52.9	0.080	3.70	9.01
		0.1 T, –0.054 mm	71.20	22.80	92.6	5.74	61.0	0.100	11.60	7.97
	1200 °C, 120 min	0.1 T, –1 mm	91.40	8.86	97.2	2.18	68.7	n/d	15.80	89.00
		0.1 T, –0.054 mm	77.80	18.90	93.5	4.93	76.9	0.066	16.60	89.40
	1200 °C, 120 min, + 15 % C	0.1 T, –1 mm	85.80	13.50	96.8	2.16	65.5	n/d	9.31	93.10
		0.1 T, –0.054 mm	65.00	31.50	89.7	7.85	80.0	0.019	14.50	92.30
N o t e: n/d – no data.										

As indicated by the data, after all types of roasting, fine grinding (–0.054 mm) leads to a significantly higher iron content in the magnetic concentrates compared to coarse grinding (–1 mm). On average, across all experiments, the iron content in the magnetic concentrates obtained after fine grinding is 11.2 % higher, and this trend is consistent for both BFS and BFD samples. However, it is important to note that due to the high cost associated with fine grinding equipment, fine grinding operations and the required significant investment for grinding [33], fine grinding does not always improve the overall efficiency of processing flowsheets. Therefore, specific technical and economic conditions of an enterprise should be considered when selecting process parameters.

Magnetic separation without preliminary roasting yielded magnetic concentrates with an iron content of 49 – 62 %, which differs insignificantly from the concentrates produced with roasting. However, the yield of the concentrates and the degree of iron recovery were relatively low, and the iron content in the non-magnetic tailings remained substantially higher. This is primarily due to the high hematite content in the initial samples. In this case, most of the zinc passed into the tailings, although the zinc content in the magnetic concentrates was only slightly lower than in the original BFS and BFD samples. These findings align with those of [19], where it was found that increasing the magnetic field strength to 0.3 T during direct magnetic separation of blast furnace sludge could improve iron recovery to 78 %. However, the study did not address the issue of increased zinc content in the magnetic separation products.

The preliminary roasting of the BFS and BFD samples at 800 °C followed by magnetic separation produced magnetic concentrates with an iron content of 51 – 61 % and an iron recovery degree of 92 – 97 %. These results differ from those of other studies, where magnetizing roasting of blast furnace dust at 600 – 800 °C with sawdust [34] and charcoal [35] was followed by magnetic separation, resulting in an iron recovery degree of approximately 85 %, which is lower than the values obtained in this study. Furthermore, those studies demonstrated that the use of sawdust or charcoal additives during the roasting enabled the transformation of a significant portion of zinc into ZnO resulting in concentrates with reduced zinc content (0.15 – 0.19 %) after magnetic separation. In contrast, despite achieving higher magnetic separation indicators in this study, no significant zinc transformation to ZnO occurred during the roasting (see Table 2). It should be noted that the most of the zinc passed into the magnetic concentrates, with the increased zinc content (0.39 – 0.43 % in the BFS sample) complicating the use of the obtained concentrates in sintering and blast furnace processes.

Thus, our study has shown that direct magnetic separation of the BFS and BFD samples, as well as the roasting-magnetic approach with carbothermic reduction at 800 °C, does not eliminate the elevated zinc content, which remains the primary challenge in processing blast furnace dust and sludge.

The metallizing roasting of the BFS and BFD samples at 1200 °C followed by magnetic separation produced magnetic concentrates with an iron content of 52 – 80 % and an iron metallization degree of 88.7 – 94.6 %, while the iron recovery in the concentrates reached 84.2 – 97.2 %. The zinc content in the concentrate obtained from the BFD sample with carbon addition was lower than in the sample without it. The zinc content of 0.048 % in the concentrates obtained from the BFS sample is below the limit for sinter product (0.05 %) allowing them to be used without issue in sintering processes.

The addition of carbon to the BFS sample did not improve the iron recovery or metallization degree in the concentrate; in fact, it slightly reduced the iron content due to the presence of excess unreacted carbon, consistent with the thermodynamic calculations (Fig. 2, *a*). In contrast, BFD processing using the roasting-magnetic method with carbon addition, followed by grinding to a particle size of –0.054 mm, resulted in an increase in both the iron content and metallization degree in the concentrate. This is likely due to the insufficient initial carbon amount in BFD to fully reduce the iron, as suggested by the absence of residual graphite in the equilibrium state after iron reduction, in contrast to the BFS case (Fig. 2, *c*). The iron content in the tailings ranged from 8.0 to 16.6 % with an iron recovery degree in the tailings of 1.9 – 8.7 % indicates the efficiency of iron extraction from blast furnace waste using the roasting and magnetic separation process.

Based on laboratory experiments, the optimal conditions for BFS and BFD processing were identified as follows: roasting at 1200 °C for 120 min, grinding the roasted samples to –0.054 mm, magnetic separation at a field strength of 0.1 T. The best magnetic separation results were observed for BFS without carbon addition and for BFD with 15 % carbon addition. Table 4 presents the chemical composition of these magnetic concentrates, while Fig. 3 illustrates their XRD patterns.

From the results obtained, it is evident that, in addition to metallic iron, the magnetic concentrates contain a considerable amount of silicates such as akermanite, gehlenite, merwinite, and anorthite, which formed during the roasting from the initial BFS and BFD components. A small amount of iron carbide was also present. The primary phase in the tailings is graphite. The concentrates and tailings also contain minor amounts of iron oxides, such as magnetite, maghemite, and hematite, which were likely formed during sample cooling due to secondary oxidation caused by the presence of oxygen impurities in the inert gas. The mineralogical composition of the

Table 4. **Chemical composition of magnetic concentrates obtained from BFS and BFD using reduction roasting and magnetic separation (roasting at 1200 °C, 120 min; grinding to –0.054 mm; magnetic separation at 0.1 T), wt. %**

Таблица 4. **Химический состав магнитных концентратов, полученных из ДШ и ДП путем восстановительного обжига и магнитной сепарации (обжиг 1200 °C, 120 мин; размол –0,054 мм; магнитная сепарация при 0,1 Тл), мас. %**

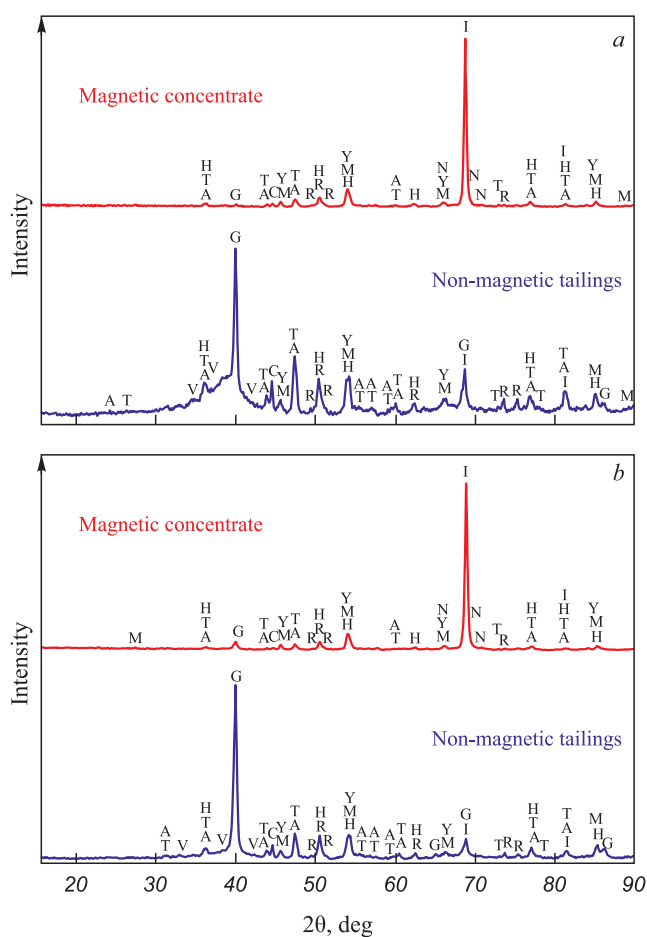| Initial sample	Content, wt. %						
	Fe	Zn	Al	Ca	Si	Mg	P
BFS	73.8	0.048	0.72	6.29	2.93	0.96	0.060
BFD + 15 % C	80.0	0.019	0.31	3.47	1.99	0.63	0.036

Fig. 3. XRD patterns of magnetic concentrate and non-magnetic tailings obtained from BFS (*a*) and BFD with 15 % C (*b*) by roasting–magnetic method (roasting at 1200 °C, 120 min; grinding to –0.054 mm; magnetic separation at 0.1 T):
I – (α-Fe); H – hematite (α-Fe_2O_3); Y – maghemite (γ-Fe_2O_3);
M – magnetite (Fe_3O_4); G – graphite (C); A – okermanite ($Ca_2MgSi_2O_7$);
T – gehlenite ($Ca_2Al_2SiO_7$); R – merwinite ($Ca_3MgSi_2O_8$);
V – anorthite ($CaAl_2Si_2O_8$); C – calcite ($CaCO_3$); N – cementite (Fe_3C)

Рис. 3. Дифрактограммы магнитного концентрата и немагнитных хвостов, полученных из ДШ (*a*) и ДП с присадкой 15 % C (*b*) обжиг-магнитным методом (обжиг 1200 °C, 120 мин; размол –0,054 мм; магнитная сепарация при 0,1 Тл):
I – (α-Fe); H – гематит (α-Fe_2O_3); Y – маггемит (γ-Fe_2O_3);
M – магнетит (Fe_3O_4); G – графит (C); A – окерманит ($Ca_2MgSi_2O_7$);
T – геленит ($Ca_2Al_2SiO_7$); R – мервинит ($Ca_3MgSi_2O_8$);
V – анортит ($CaAl_2Si_2O_8$); C – кальцит ($CaCO_3$);
N – цементит (Fe_3C)

concentrate and tailings obtained from the BFS and BFD samples shows only slight differences.

After the roasting and magnetic separation under the conditions above, the magnetic concentrate with low zinc content can be recycled as part of the sinter burden. The zinc-containing sublimate obtained during the reduction roasting can be considered as a raw material for zinc production, while the non-magnetic tailings obtained during magnetic separation can be used as a raw material in the production of construction materials. Another option is to bypass the magnetic separation stage after the reduction roasting of BFS and BFD, which would avoid the costly grinding of the roasted product and allow the direct recycling in sinter production. However, this would result in the introduction of gangue into the blast furnace charge. A significant advantage of the obtained concentrates is the high reduced iron content, which accelerates the agglomeration process. The use of such concentrates in sinter production reduces the consumption of coke and lime, enables waste recycling, and decreases the need for natural iron-containing raw materials.

It is also worth noting that the metallized concentrates could potentially be used as a charge for electric arc furnace smelting. However, the concentrates do not currently meet the requirements of existing enterprises [36], which include % $Fe_{tot} \geq 88$, % $Fe_{met} \geq 79$, iron metallization degree ≥ 90 %, % $P \leq 0.015$, % $Si \leq 0.5$. In order to evaluate the feasibility of using these concentrates in steelmaking, further industrial testing is needed, along with possible adjustments to metallized raw material requirements for EAF smelting and improvements in the roasting and magnetic separation processes for blast furnace dust and sludge.

CONCLUSIONS

The study has shown that the optimal solution for processing BFS and BFD samples is preliminary magnetizing roasting at 1200 °C for 120 min, followed by grinding to –0.054 mm and magnetic separation with a magnetic field of 0.1 T. This process resulted in a dezinced magnetic concentrate from BFS with an iron content

of 73.8 %, an iron metallization degree of 88.9 %, and an iron recovery degree of 92.8 %. For BFD, the addition of 15 % carbon produced a dezinced magnetic concentrate with an iron content of 80 %, an iron metallization degree of 92.3 %, and an iron recovery degree of 89.7 %.

▮ REFERENCES / СПИСОК ЛИТЕРАТУРЫ

1. Omran M., Fabritius T., Paananen T. Effect of blast furnace sludge (BFS) characteristics on suitable recycling process determining. *Journal of Minerals and Materials Characterization and Engineering.* 2017;5(4):185–197. https://doi.org/10.4236/jmmce.2017.54016

2. Jiao K.X., Zhang J.L., Liu Z.J., Chen C.L., Liu F. Circulation and accumulation of harmful elements in blast furnace and their impact on the fuel consumption. *Ironmaking and Steelmaking.* 2017;44(5):344–350. https://doi.org/10.1080/03019233.2016.1210913

3. Letimin V.N., Nasyrov T.M., Makarova I.V. Evaluation of pyrometallurgical methods for dezincification of dust and sludge from steelmaking workshops. *Teoriya i tekhnologiya metallurgicheskogo proizvodstva.* 2013;(1(13)):67–70. (In Russ.).

    Летимин В.Н., Насыров Т.М., Макарова И.В. Оценка пирометаллургических способов обесцинкования пыли и шламов сталеплавильных цехов. *Теория и технология металлургического производства.* 2013;(1(13)):67–70.

4. Baidya R., Kumar Ghosh S., Parlikar U.V. Blast furnace flue dust co-processing in cement kiln – A pilot study. *Waste Management and Research.* 2019;37(3):261–267. https://doi.org/10.1177/0734242X18816791

5. Francis A.A. Crystallization kinetics of magnetic glass-ceramics prepared by the processing of waste materials. *Materials Research Bulletin.* 2006;41(6):1146–1154. https://doi.org/10.1016/j.materresbull.2005.11.002

6. López-Díaz A., Ochoa-Díaz R., Grimaldo-León G.E. Use of BOF slag and blast furnace dust in asphalt concrete: An alternative for the construction of pavements. *DYNA (Colombia).* 2018;85(204):24–30. https://doi.org/10.15446/dyna.v85n206.70404

7. Díaz R.O., Rojas A.P., León G.G. Use of blast furnace dust in the production of asphalt concrete for pavements, performance and environmental contribution. *Journal of Sustainable Architecture and Civil Engineering.* 2023;32(1):224–232. https://doi.org/10.5755/j01.sace.32.1.32300

8. Xie B., Geng N., Yu Q., He D., Wang F., Liu T., Gao J., Ning P., Song X., Jia L. Removal of SO_2 from flue gas using blast furnace dust as an adsorbent. *Environmental Science and Pollution Research.* 2022;29:15642–15653. https://doi.org/10.1007/s11356-021-16842-7

9. Carrillo Pedroza F.R., Soria Aguilar M. de J., Sánchez Castillo M.A., Martínez Luévanos A., Picazo Rodríguez N.G. Adsorption of chromium from steel plating wastewater using blast furnace dust. *Revista Internacional de Contaminacion Ambiental.* 2017;33(4):591–603. https://doi.org/10.20937/RICA.2017.33.04.04

10. Liu S., Zhou W., Niu S., Han K., Wang Y., Lu C, Li Y., Wang J. Insight into blast furnace dust for selective catalytic reduction of NO_x: An experimental and DFT study. *Fuel.* 2023;344:128006. https://doi.org/10.1016/j.fuel.2023.128006

11. Mu Y., Liang X., Wu M., Li C., Xia T., Chen K., Li X. Utilizing blast-furnace dust as a novel persulfate catalyst for the efficient removal of petroleum contaminants from soil. *Journal of Cleaner Production.* 2024;434:140112. https://doi.org/10.1016/j.jclepro.2023.140112

12. Zhang Y., Li S., Wang X., Li X. Coagulation performance and mechanism of polyaluminum ferric chloride (PAFC) coagulant synthesized using blast furnace dust. *Separation and Purification Technology.* 2015;154:345–350. https://doi.org/10.1016/j.seppur.2015.09.075

13. Xiao X., Zhang S., Sher F., Chen J., Xin Y., You Z., Wen L., Hu M., Qui G. A Review on recycling and reutilization of blast furnace dust as a secondary resource. *Journal of Sustainable Metallurgy.* 2021;7:340–357. https://doi.org/10.1007/s40831-021-00377-9

14. Zeydabadi B.A., Mowla D., Shariat M.H., Kalajahi J.F. Zinc recovery from blast furnace flue dust. *Hydrometallurgy.* 1997;47(1):113–125. https://doi.org/10.1016/S0304-386X(97)00039-X

15. Soria-Aguilar M.D.J., Davila-Pulido G.I., Carrillo-Pedroza F.R., Gonzalez-Ibarra A.A., Picazo-Rodriguez N., Lopez-Saucedo F.D.J., Ramos-Cano, J. Oxidative leaching of zinc and alkalis from iron blast furnace sludge. *Metals (Basel).* 2019;9(9):1015. https://doi.org/10.3390/met9091015

16. Zhang J.X., Niu F.S., Li L., Xie J. Beneficiability study of the blast furnace dust from Tangshan iron and steel company. *Advanced Materials Research.* 2013;712–715:420–423. https://doi.org/10.4028/www.scientific.net/AMR.712-715.420

17. Lanzerstorfer C. Air classification of blast furnace dust catcher dust for zinc load reduction at the sinter plant. *International Journal of Environmental Science and Technology.* 2016;13:755–760. https://doi.org/10.1007/s13762-015-0903-1

18. Tripathy S.K., Jaiswal S., Rama Murthy Y., Nag S. Separation analysis of flotation to recover the carbon values from blast furnace gas cleaning plant sludge. *Metallurgical Research & Technology.* 2016;113(3):303. https://doi.org/10.1051/metal/2016011

19. Jena M.K., Mahanta J., Mahapatra M.M., Baliarsingh M., Mishra S. Recovery of iron values from blast furnace gas cleaning process sludge by medium intensity magnetic separation method. In: *Recent Advances in Mechanical Engineering. Lecture Notes in Mechanical Engineering.* Pradhan P., Pattanayak B., Das H.C., Mahanta P. eds. Singapore: Springer; 2023:449–454. https://doi.org/10.1007/978-981-16-9057-0_48

20. Das B., Prakash S., Reddy P.S.R., Biswal S.K., Misra V.N. Effective utilization of blast furnace flue dust of integrated steel plants. *The European Journal of Mineral Processing and Environmental Protection.* 2002;2(2):61–68.

21. Yehia A., El-Rahiem F.H. Recovery and utilization of iron and carbon values from blast furnace flue dust. *Mineral Processing and Extractive Metallurgy.* 2005;114(4):207–211. https://doi.org/10.1179/037195505X28519

22. Deng X., Huang R., Lv X., Yang J., Yang J. Separation and recovery of metallic zinc and iron concentrate from blast furnace dust by vacuum carbothermal reduction. *Process Safety and Environmental Protection.* 2022;162:746–751. https://doi.org/10.1016/j.psep.2022.04.050

23. Luo L., Zhang X., Wang H., Zheng B., Wei C. Comparing strategies for iron enrichment from Zn- and Pb-bearing refractory iron ore using reduction roasting-magnetic separation. *Powder Technology.* 2021;393:333–341. https://doi.org/10.1016/j.powtec.2021.07.085

24. Xu X., Guo Z., Zhu D., Pan J., Yang C., Li S. Application of coal-based direct reduction-magnetic separation process for recycling of high-iron-content non-ferrous metallurgical wastes: Challenges and opportunities. *Process Safety and Environmental Protection*. 2024;183:59–76. https://doi.org/10.1016/j.psep.2023.12.057

25. Putz H., Brandenburg K. Match! – Phase identification from powder diffraction, version 3.15, Crystal Impact, Bonn 2023. Available at URL: https://www.crystalimpact.de/match (Accessed 12.09.2024).

26. Roine A. HSC Chemistry® software, version 9.9, Outotec, Pori, Finland 2019. Available at URL: https://www.outotec.com/HSC (Accessed 12.09.2024).

27. Sun Y., Zhu X., Han Y., Li Y. Green magnetization roasting technology for refractory iron ore using siderite as a reductant. *Journal of Cleaner Production*. 2019;206:40–50. https://doi.org/10.1016/j.jclepro.2018.09.113

28. Li C., Sun H., Bai J., Li L. Innovative methodology for comprehensive utilization of iron ore tailings. Part 1. The recovery of iron from iron ore tailings using magnetic separation after magnetizing roasting. *Journal of Hazardous Materials*. 2010;174(1-3):71–77. https://doi.org/10.1016/j.jhazmat.2009.09.018

29. Zhao Q., Xue J., Chen W. A Novel self-magnetizing roasting process for recovering Fe from low-grade pyrite cinder and blast furnace sludge. *Transactions of the Indian Institute of Metals*. 2019;72:2547–2556. https://doi.org/10.1007/s12666-019-01724-x

30. Chen B., Yi X., Zhan W., Gao L., He Z., Zhang J. Pyrometallurgical recovery of zinc and valuable metals from hazardous blast furnace dust via self-reduction roasting: Phase transformations and morphological evolution. *Materials Today Sustainability*. 2023;24:100590. https://doi.org/10.1016/j.mtsust.2023.100590

31. Filippova N.A. Phase Analysis of Ores and Products of their Processing. Moscow: Khimiya; 1975:111. (In Russ.).

Филиппова Н.А. Фазовый анализ руд и продуктов их переработки. Москва: Химия; 1975:111.

32. Roy S.K., Nayak D., Rath S.S. A review on the enrichment of iron values of low-grade Iron ore resources using reduction roasting-magnetic separation. *Powder Technology*. 2020;367:796–808. https://doi.org/10.1016/j.powtec.2020.04.047

33. Yagupov A.V., Zamytskii V.S., Klykov Yu.G., Zamytskii O.V. Increasing the efficiency of ore processing. *Gornyi informatsionno-analiticheskii byulleten'*. 1997;(2):163–165. (In Russ.).

Ягупов А.В., Замыцкий В.С., Клыков Ю.Г., Замыцкий О.В. Повышение эффективности переработки руд. *Горный информационно-аналитический бюллетень*. 1997;(2):163–165.

34. Wang B., Feng Y., Li H., Ju J., Yang Y. Separation of iron and zinc values from blast furnace dust adopting reduction roasting-magnetic separation method by sawdust pyrolysis. *Mining, Metallurgy & Exploration*. 2023;40:1357–1368. https://doi.org/10.1007/s42461-023-00803-4

35. Ju J., Feng Y., Li H., Zhang Q. Study of recycling blast furnace dust by magnetization roasting with straw charcoal as reductant. *Physicochemical Problems of Mineral Processing*. 2022;58(3):149265. https://doi.org/10.37190/ppmp/149265

36. Medenkov S.A. Promising use of metallized pellets in electrometallurgy. In: *Materials of the 66th Sci. Conf. Science of SUSU. Sections of Technical Sciences*. Chelyabinsk: SUSU; 2014:1404–1410. (In Russ.).

Меденков С.А. Перспективное использование металлизированных окатышей в электрометаллургии. В кн.: *Материалы 66-й научной конференции Наука ЮУрГУ. Секции технических наук*. Челябинск: ИД ЮУрГУ; 2014:1404–1410.

Information about the Authors / Сведения об авторах

Pavel I. Grudinsky, *Junior Researcher of the Bardin Laboratory of Metallurgy of Complex Ores,* Baikov Institute of Metallurgy and Materials Science, Russian Academy of Sciences
ORCID: 0000-0002-7358-150X
E-mail: pgrudinskiy@imet.ac.ru

Anfisa A. Yurtaeva, *Senior Laboratory Research Assistant of the Bardin Laboratory of Metallurgy of Complex Ores,* Baikov Institute of Metallurgy and Materials Science, Russian Academy of Sciences
ORCID: 0009-0005-4449-2208
E-mail: anfisayurtaeva@mail.ru

Anton I. Volkov, *Cand. Sci. (Chem.), Director of N.P. Lyakishev Scientific Center of Complex Processing of Raw Materials,* I.P. Bardin Central Research Institute of Ferrous Metallurgy
ORCID: 0000-0003-1777-3889
E-mail: rhenium@list.ru

Valerii G. Dyubanov, *Cand. Sci. (Eng.), Leading Researcher of the Bardin Laboratory of Metallurgy of Complex Ores,* Baikov Institute of Metallurgy and Materials Science, Russian Academy of Sciences
ORCID: 0009-0001-5830-7799
E-mail: vdyubanov@imet.ac.ru

Павел Иванович Грудинский, *младший научный сотрудник лаборатории проблем металлургии комплексных руд им. академика И.П. Бардина,* Институт металлургии и материаловедения им. А.А. Байкова РАН
ORCID: 0000-0002-7358-150X
E-mail: pgrudinskiy@imet.ac.ru

Анфиса Александровна Юртаева, *старший лаборант-исследователь лаборатории проблем металлургии комплексных руд им. академика И.П. Бардина,* Институт металлургии и материаловедения им. А.А. Байкова РАН
ORCID: 0009-0005-4449-2208
E-mail: anfisayurtaeva@mail.ru

Антон Иванович Волков, *к.х.н., директор Научного центра комплексной переработки сырья им. Н.П. Лякишева,* Центральный научно-исследовательский институт черной металлургии им. И.П. Бардина
ORCID: 0000-0003-1777-3889
E-mail: rhenium@list.ru

Валерий Григорьевич Дюбанов, *к.т.н., ведущий научный сотрудник лаборатории проблем металлургии комплексных руд им. академика И.П. Бардина,* Институт металлургии и материаловедения им. А.А. Байкова РАН
ORCID: 0009-0001-5830-7799
E-mail: vdyubanov@imet.ac.ru

Contribution of the Authors / Вклад авторов

P. I. Grudinsky – conceptualization, writing the text, conducting thermodynamic calculations and laboratory experiments, titrimetric iron analysis, processing and analysis of the results.

A. A. Yurtaeva – conducting laboratory experiments, titrimetric iron analysis, editing the text.

A. I. Volkov – *X*-ray fluorescence analysis, editing the text.

V. G. Dyubanov – scientific guidance, editing the text.

П. И. Грудинский – разработка концепции работы, написание текста статьи, выполнение термодинамических расчетов и лабораторных экспериментов, титриметрическое определение железа, обработка и анализ результатов.

А. А. Юртаева – выполнение лабораторных экспериментов, титриметрическое определение железа, редактирование текста статьи.

А. И. Волков – рентгенофлуоресцентный анализ, редактирование текста статьи.

В. Г. Дюбанов – научное руководство, редактирование текста статьи.